

# A Comparison of Phase Space Reconstruction and Spectral Coherence Approaches for Diagnostics of Bar and End-Ring Connector Breakage Faults in Polyphase Induction Motors using Current Waveforms

Richard J. Povinelli<sup>1</sup>, Michael T. Johnson<sup>1</sup>, John F. Bangura<sup>2</sup>, Nabeel A.O. Demerdash<sup>1</sup>

<sup>1</sup>Department of Electrical and Computer Engineering  
Marquette University, 1515 W. Wisconsin Ave.  
Milwaukee, WI 53233  
{richard.povinelli, mike.johnson,  
nabeel.demerdash}@marquette.edu

<sup>2</sup>Black & Decker  
701 East Joppa Road, TW100  
Towson, MD 21286  
john.bangura@bdk.com

**Abstract** – Two signal (waveform) analysis approaches are investigated in this paper for motor-drive fault identification – one linear and the other nonlinear. Twenty-one different motor-drive operating conditions including healthy, 1 through 10 broken bars, and 1 through 10 broken end-ring connectors are investigated. Highly accurate numerical simulations of current waveforms for the various operating conditions are generated using the Time Stepping Coupled Finite Element – State Space method for a 208-volt, 60-Hz, 2-pole, 1.2-hp, squirrel cage 3-phase induction motor. The linear signal analysis method is based on spectral coherence, whereas the nonlinear signal analysis method is based on stochastic models of reconstructed phase spaces. Conclusions resulting from the comparisons of these two methods are drawn.

**Keywords** – *Fault diagnosis, induction motors, electric drives, time stepping finite elements, state space methods, spectral coherence, dynamical systems analysis.*

## I. INTRODUCTION

Induction machine adjustable speed drives (IMASDs) are popular motor-drive systems for a wide range of applications throughout the manufacturing, processing, energy, transportation, service, and medical industries. Applications of electric motor drives include among other things, material processing and handling, medical systems, electromechanical automation, propulsion and actuation, fluid flow systems, heating and air-conditioning systems, as well as in automotive, marine, and aerospace applications. The reliability of these drives can be critical. Drive failure may lead to plant shut down and resulting long repair cycle or even to major industrial accidents in mission critical applications. Fault identification and diagnostics can improve reliability by identifying incipient faults before major drive failure occurs, allowing drive repair/replacement to occur in a timely and orderly fashion.

Given the importance of fast and accurate motor-drive diagnostic tools, this paper investigates two approaches to signal analysis – one linear and the other nonlinear – to identifying 21 different motor-drive configurations including: healthy, 1 through 10 broken bars, and 1 through 10 broken end-ring connectors. This is done using highly accurate numerical simulations of the current waveforms for the various operating conditions generated using the Time Stepping Coupled Finite Element – State Space (TSCFE-SS) method [1-5] for a 208-volt, 60-Hz, 2-pole, 1.2-hp, squirrel cage 3-phase induction motor. The linear signal method, based on spectral coherence, and nonlinear signal analysis method, based on stochastic models of reconstructed phase spaces, are compared and contrasted.

A comprehensive survey of the literature of motor-drive diagnostics was undertaken by Benboizid [6]. As stated in [6], “performing reliable and accurate fault detection and diagnosis requires understanding the cause and effect of motor faults to motor performances.” The purpose of research in the area of fault signature analysis is to help understand this “cause and effect” and to develop methods for automatically recognizing faults, characterizing the fault types, and eventually for predicting the onset of these faults. Current methods for classification of fault types are primarily based on frequency-domain analysis of the signal harmonics, usually taken over a relatively large number of cycles in order to obtain sufficient frequency resolution. Classification approaches using such spectral features have included statistical pattern recognition using Naïve Bayes classifiers [7] as well as non-linear classifiers such as neural networks [8].

In our previous work in motor-drive diagnostics [9-11], a nonlinear phase space reconstruction method called Time Series Data Mining (TSDM) was used to classify with 100% accuracy 13 different motor operating characteristics. Using the torque profile generated by the TSCFE-SS method for each operating condition, a reconstructed two-dimensional

phase space was created. We then computed the first and second order statistical features of the projected state trajectory. These two features were used in a nearest neighbor learner and tested with 100% accuracy on sets of out of sample data of the torque profiles. These results showed that this method was capable of differentiating even among difficult motor faults such as amongst the four types of eccentricities dealt with in [9-11].

The most obvious drawback of the reliance on the torque profile as the input to the diagnostic system is the requirement of a torque transducer in an actual drive with its associated added costs and other motor-drive user concerns. Such cost could be justified in large and mission critical motor-drive systems where the additional cost of torque transducer would be relatively insignificant to the total cost of the system. Hence, it would be worth the additional information provided by the torque transducer in mission critical scenarios.

Here, in order to address this drawback, we use the current waveforms and investigate a more sophisticated characterization of the phase space using techniques pioneered in the biomedical field for heart arrhythmia classification [12]. Additionally, we compare the nonlinear signal analysis method with a linear signal analysis approach, which uses spectral features such as coherence.

The paper consists of five parts. The second section presents the TSCFE-SS method for generating operating characteristics of a great variety of motor-drive operating conditions. The third section discusses the reconstructed phase space based technique. The fourth section discusses the frequency analysis (spectral) approach. The fifth section presents the data and experimental design. The final section compares the results of these two approaches.

## II. TIME STEPPING COUPLED FINITE ELEMENT – STATE SPACE (TSCFE-SS) METHOD

The TSCFE-SS method computes in sampled data form the time-domain waveforms and profiles of the input phase and line currents, voltages, developed power and torque of a motor as function of the particular magnetic circuit, winding layouts, and materials as well as inverter (controller) topology and operating conditions. These types of simulations can include faulty operating conditions such as open or short-circuited portions of windings, breakages in squirrel-cage bars and end-ring connectors, shaft/rotor dynamic and static eccentricities, as well as faults within inverter topologies such as malfunctioning switching. Computations and simulations include the full effects of interaction of machine space harmonics with time-domain harmonics caused by the electronic switching on the overall motor-controller/drive performances [5, 13].

The TSCFE-SS modeling and simulation fully incorporates in rigorous and intricate detail the nonlinear effects of magnetic saturation in the machine, including the peculiar saturation patterns that result in a machine’s magnetic circuit due to winding and squirrel-cage faults. Thus, the full impact of these uneven and unusual saturation patterns on terminal current and voltage waveforms and motor torque profiles is included in the simulations; see references [5, 13]

for details. The TSCFE-SS formulation is fully based on the natural machine windings flux linkage frame of reference, and thus the machine-controller models are fully integrated; see references [5, 13] for details.

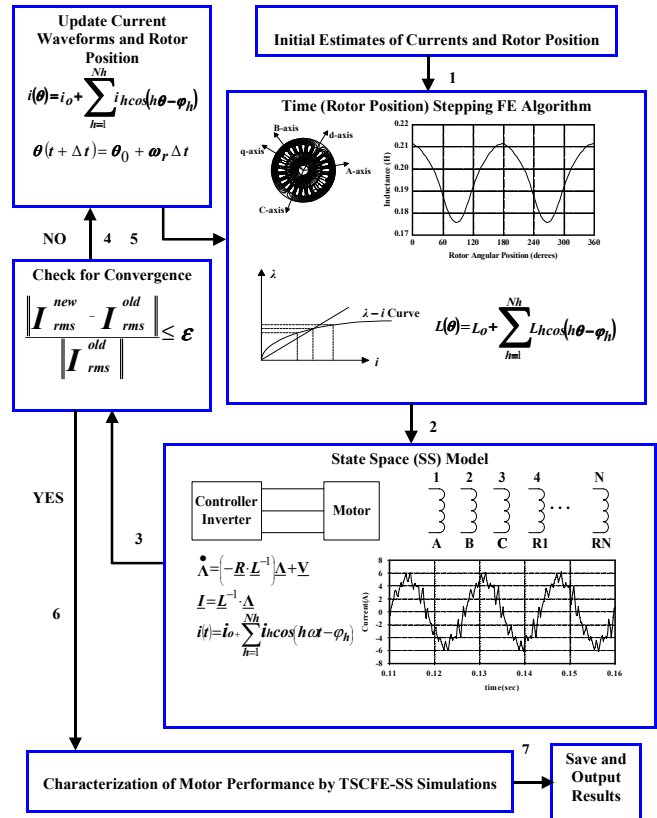


Figure 1 – Functional Block-Diagram/Flow Chart of the TSCFE-SS Method

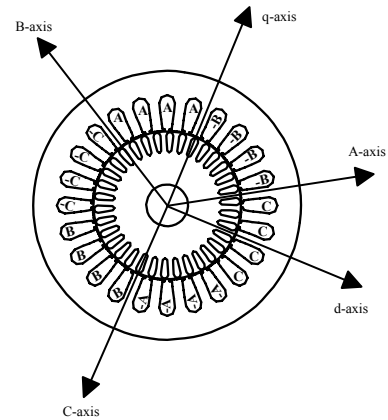
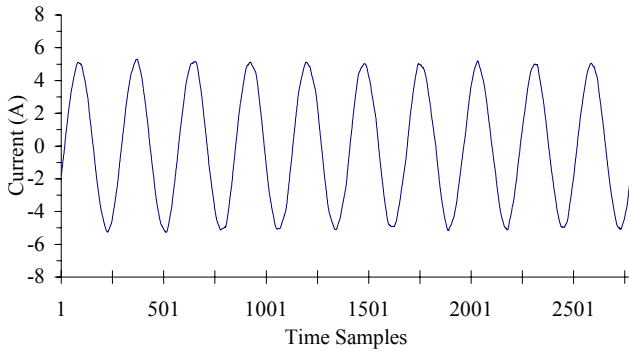


Figure 2 - Motor Cross Section

Also, see Figure 1 for the functional flow chart block diagram, which summarizes the essence of this machine-controller modeling and simulation method. Details of how this simulation technique can model motor faults such as squirrel-cage bar and end-ring connector breakages, as well as dynamic and static eccentricities were given earlier in reference [9-11]. Thus, this modeling and simulation technique and algorithm here constitutes the “engine” through which the databases on faulty motor winding current, voltage,

and developed torque waveforms/profiles are generated for the faults under study in this paper. The algorithm was applied to squirrel-cage breakages in a 1.2-hp, 120-volt, 3-phase, 2-pole, and 34-squirrel-cage bar induction motor whose cross-section is given in Figure 2.

As illustrative examples of the output of the TSCFE-SS simulations used in this paper, the current waveforms generated for the healthy and 1, 3, and 6 broken bars are given in Figures 3, 4, 5, and 6, respectively.



**Figure 3 – Healthy Motor Current Waveform**

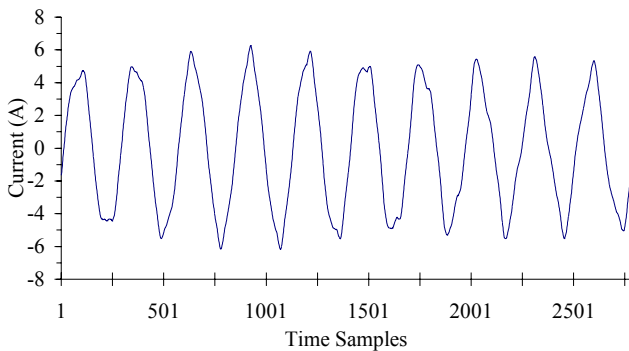


**Figure 4 – One Broken Bar Current Waveform**

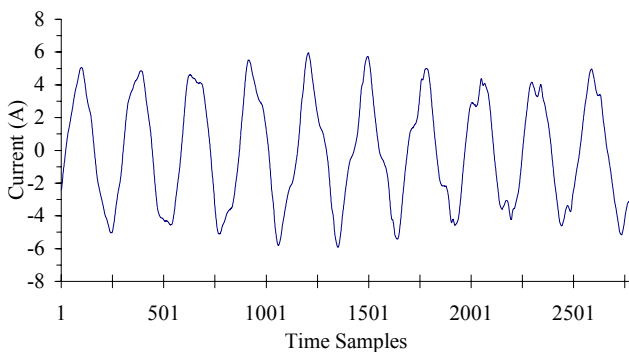


**Figure 5 – Three Broken Bars Current Waveform**

### III. PHASE SPACE RECONSTRUCTION METHOD

The current waveforms given in Figures 3 through 6 are input to a phase space based classifier system for fault diagnostics. This classifier system is based on discrete stochastic models of reconstructed phase spaces. This approach is a new nonlinear signal analysis method based on dynamical systems theory.

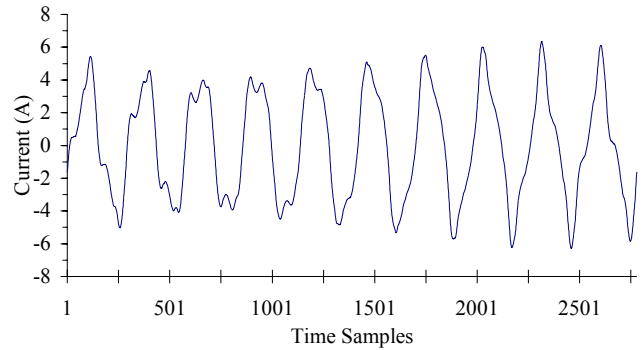


**Figure 6 – Six Broken Bars Current Waveform**

The theoretical justification for this approach comes from Takens' Theorem [14], in which it is shown that a topologically equivalent state space can be recovered from a single sampled state variable. This means that the dynamical invariants are also maintained [15]. Hence, from the current waveforms generated by a motor-drive system, an equivalent to the original state information can be recovered. This recovered state information would allow exact determination of the structure of the motor, hence a database of the state structures for various motor configurations could be constructed to which unknown motors could be compared for fault classification. The theory requires assumption that in practice cannot be met, such as infinite signal length, noise free signals, and known dimension of the original system. Given that the original simulations use a 37<sup>th</sup> order state model, a 75<sup>th</sup> dimension reconstructed phase space would be required. Fortunately, the theoretically sufficient conditions do not imply practical necessary conditions, especially for signal classification problems. In practice far smaller phase spaces are required.

There are two parameters that must be learned to form a reconstructed phase space from a signal. These parameters are the time lag and the dimension. The standard method used to determine the time lags is based on automutual information [16]. This is an information theoretic measure that determines the amount of shared information between two time lags. The first minimum of the automutual information function is used as the lag. The standard method for determining the reconstructed phase space dimension is the false nearest neighbor method [16], which measures the percentage of points that are projected close, rather than are close because of the dynamics of the system.

In previous work [9] discussed above, we used first and second order statistical characterizations of the reconstructed phase space of torque profiles as features for a nearest neighbor learner. The new approach [12] described here estimates a probability mass function as a model of the reconstructed phase space. The estimates of the probability masses form the feature set for a nearest neighbor learner [17].

Examining the reconstructed phase spaces can also motivate the reconstructed phase space based approach. The first step is to take the first difference of the current waveforms. This is a standard time series analysis technique [18]. We have found it useful in our previous fault diagnostic

work with motor data [9, 19]. The current first difference is defined as follows

$$\Delta i = i(k) - i(k-1), \quad (1)$$

where  $i(k)$  is the current waveform, and  $k$  is a time index.

A two dimensional reconstructed phase space is created by plotting  $\Delta i(k-26)$  on the x-y plane's abscissa and  $\Delta i(k)$  on the ordinate. The standard automutual information method is used to determine the time lag of 26. Figures 7, 8, 9, and 10 illustrate the two-dimensional reconstructed phase spaces of the healthy, one broken bar, three broken bars, six broken bars, and nine broken bars current first differences, respectively. They are direct transformations of the current waveforms illustrated in Figures 3, 4, 5, and 6. We can see that even with a two dimensional reconstructed phase space, the trajectories differ such that visual differences can be easily observed. The purpose of the proposed method is to capture the visual differences with a set of features.

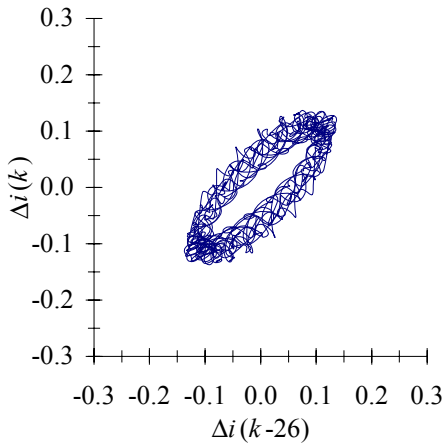


**Figure 7 – Healthy Current First Difference Phase Space**

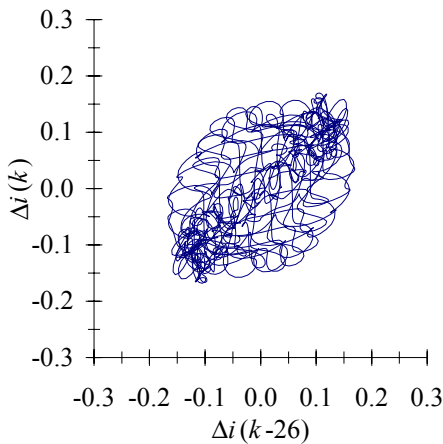


**Figure 8 – One Broken Bar Current First Difference Phase Space**

The method to capture these differences is comprised of three major steps. The first step is to determine the time lags and reconstructed phase space dimension. This is done using the automutual information technique and the false nearest neighbor method discussed above. The TISEAN software was

used for these calculations [20]. The first minima of the automutual information function were 24, 38, 26, 32, and 26 for the healthy, one broken bar, three broken bars, six broken bars, and nine broken bars current first differences waveforms, respectively. The median of 26 was selected as the lag. Other lags were examined for their impact on the dimension returned by the false nearest neighbor method, but the selected lag of 26 provided the best performance. Using the lag of 26 as an input to the false nearest neighbor method, the best false nearest neighbor dimensions were 5, 5, 4, 4, and 4 for the healthy, one broken bar, three broken bars, six broken bars, and nine broken bars current first differences waveforms, respectively. For the healthy motor there were 0.03% false nearest neighbors at dimension 5 and for the one broken bar there were 0.06% false nearest neighbors at dimension 5, so a dimension of 4 was used for the reconstructed phase spaces.

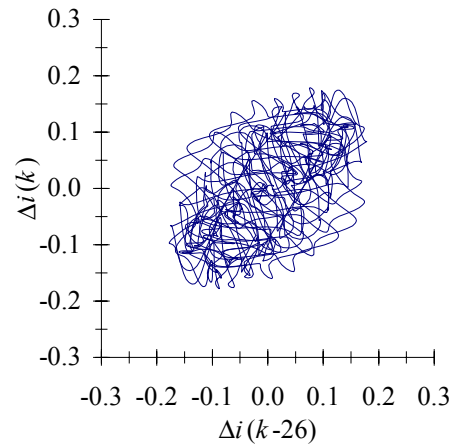


**Figure 9 – Three Broken Bar Current First Difference Phase Space**

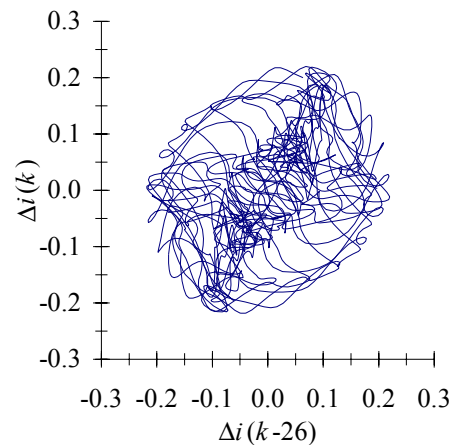


**Figure 10 – Six Broken Bar Current First Difference Phase Space**

The second step is to determine the regions from which the probability mass function will be estimated. This is done by partitioning each dimension of the reconstructed phase space into four strips. This is illustrated in two dimensions in Figure 11. The intercepts that define the strips are learned from all the training examples such that each strip will contain

approximately the same occurrence of phase space points. Next, the probability mass function is learned for each training signal. These probability mass functions form the models to which new signals will be compared for classification.

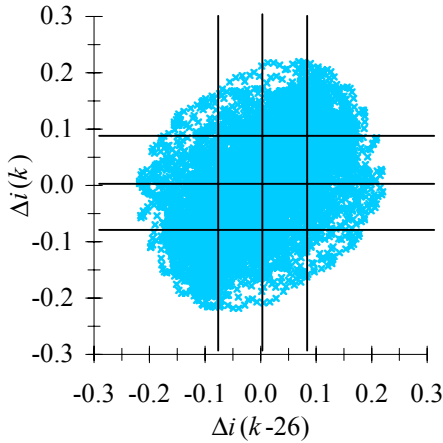


**Figure 11 – Phase Space Partitioning**

The third step is to classify new test signals. This is done by first estimating the probability mass function of the new signal for its reconstructed phase space. The test reconstructed phase space is compared against each of the templates learned in the training phase using the Bhattacharyya distance [21].

$$d(a,b) = -\ln\left(\sum_{i=1}^N \sqrt{a_i b_i}\right), \quad (2)$$

where  $a_i$  is the probability mass for a partition of the test signal,  $b_i$  is the probability mass for a partition of a training signal, and  $N$  is the number of partitions. Examples of these partitions are illustrated in Figure 11. The test signal is assigned the class label of the nearest training signal according to the Bhattacharyya distance.

#### IV. SPECTRAL COHERENCE METHOD

We now compare the classification features based on the phase space reconstruction method to those based on traditional spectrally motivated features using signal-processing techniques. To do this, we have constructed a similarity measure using spectral coherence [22] and applied it to the same current first difference waveforms used for phase space reconstruction. This approach is advantageous in that it allows a direct comparison of the frequency content between two different waveforms, does not rely on an explicit model of the underlying signal harmonics, and may be implemented on shorter signal windows than would be acceptable when doing the high-resolution analysis required for computing sideband amplitudes, such as [7, 8].

Spectral coherence is the normalized cross-power spectrum [22] computed between two signals  $X$  and  $Y$ , given by:

$$C_{XY}(\omega) = \frac{|P_{XY}(\omega)|^2}{P_{XX}(\omega)P_{YY}(\omega)} \quad (3)$$

where  $C_{XY}$  is coherence,  $P_{XY}$  is cross power spectral density, and  $P_{XX}$  and  $P_{YY}$  are the power spectral densities of  $X$  and  $Y$  respectively. Here,  $X$  and  $Y$  are the current first differences of the two motor waveforms to be compared. Welch's average periodogram method [23] is used to compute the coherence, with overlapping Blackman windows and a 2-cycle window length, thus resulting in a 30Hz frequency resolution characteristic.

There are several metrics that could be used to combine the coherence spectrum into a single measure of similarity between two waveforms. One such measure would simply be the sum of the spectral coherence over a particular frequency range of interest. Other measures based on coherence across the entire spectrum or on additional analysis of the coherence spectrum are also possible. For this work, we have used a simple coherence sum at all 60Hz harmonics, starting with the second harmonic. Classification is accomplished using a simple nearest neighbor algorithm [17], by computing the coherence sum of a given test signal with each training example, and choosing the fault type of the training signal with the highest coherence.

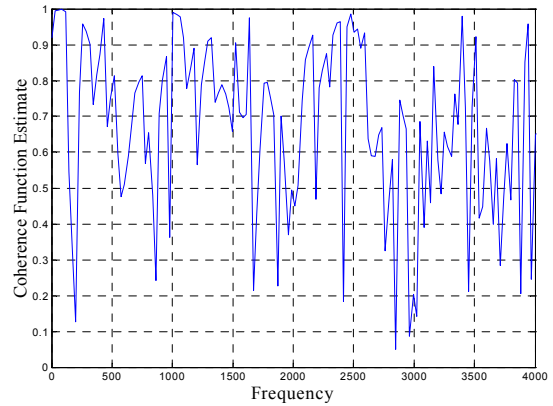


**Figure 12 - Healthy-Healthy Coherence Spectrum**

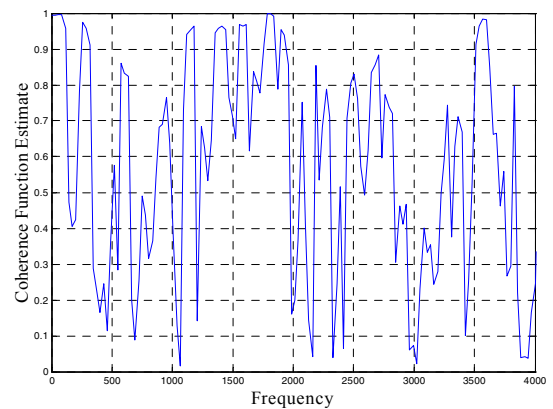


**Figure 13 - Healthy - 1 Broken Bar Coherence Spectrum**

Figures 12 through 14 show example coherence spectra between a healthy motor segment and several training waveforms, including another healthy segment as well as one broken bar and six broken bar fault scenarios. The plots indicate differences within the structure of the coherence

spectra and also a generally higher coherence between the segments of the same type.

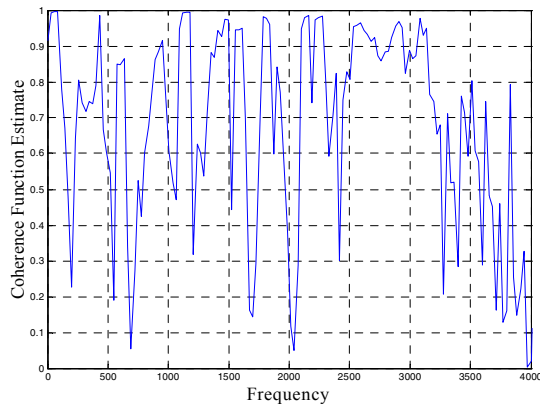


Figure 14 - Healthy - 6 Broken Bar Coherence Spectrum

### V. DATA AND EXPERIMENTAL DESIGN

The data set consists of 5 cycle segments taken from the first difference of the steady state current simulations. A total of 20 segments from each operating mode (healthy, 1-10 broken bars, 1-10 broken connectors) were used for these experiments. The data was divided into training and testing sets using a tenfold cross validation approach, giving ten independent experimental runs where each run consisted of 90% of the waveform segments being used for training and 10% of the segments being reserved for testing. Overall results were compiled into a single accuracy number.

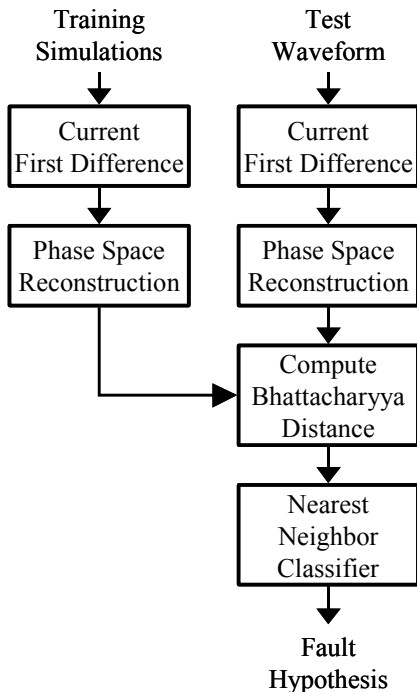


Figure 15 - Block diagram of phase space reconstruction method for fault identification

Each of the proposed methods were used to implement a simple nearest neighbor classifier based on the distance metrics described in the two preceding sections,

Bhattacharyya distance in the case of phase space reconstruction and summed harmonic coherence in the case of the coherence-based method. Classification is thus accomplished by comparing each test segment to all of the training segments and selecting the class corresponding to the closest of these. Block diagrams summarizing each of the two approaches are shown in Figures 15 and 16.

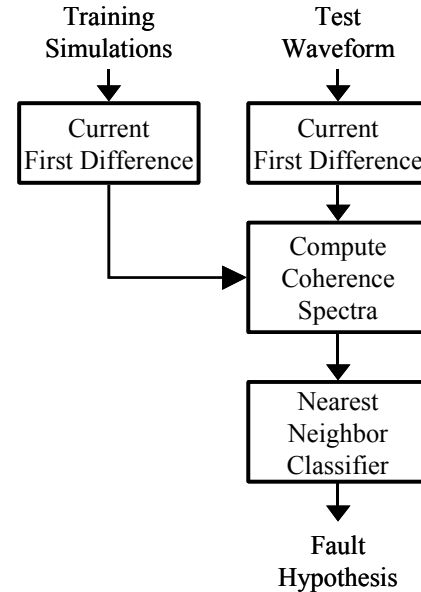


Figure 16 - Block diagram of coherence spectrum method for fault identification

Each of the methods resulted in 100% accuracy over the simulated waveform test set. It should be noted that the simulated data waveforms are for static speed and load conditions and are also unaltered by measurement noise that would exist with current sensors in the field, so that such high accuracies in the field are probably not achievable. However, the results do indicate great promise for very fast response fault identification methods, which require relatively short analysis windows and are free of the need for explicit sideband harmonic models or estimates.

### VI. CONCLUSIONS

In our previous work [9], we used the torque profile as input to the fault identification algorithm. In that work [9], 100% accuracy was achieved in classifying 12 operating conditions studied using first and second order statistical characterizations of the reconstructed phase space. The drawback to using the torque profile is the added cost of a torque transducer in an actual motor-drive, hence in this paper we investigated using the current waveform as the input to two different fault identification algorithms.

Both the linear signal analysis and nonlinear signal analysis algorithms were capable of classifying all 21 operating conditions. Advantages of these methods over those based on harmonic sideband models include in particular the capability for operating on short analysis windows, thus allowing faster response time for identifying faults.

## REFERENCES

- [1] J. F. Bangura and N. A. Demerdash, "Performance and Torque-Ripple Characterization in Induction Motor Adjustable Speed Drives Using Time-Stepping Coupled Finite Element State Space Techniques," *IEEE Transactions on Industry Applications*, vol. 35, pp. 982-990, 1999.
- [2] N. A. O. Demerdash and J. F. Bangura, "Characterization of Induction Motors in Adjustable-Speed Drives Using a Time-Stepping Coupled Finite-Element State-Space Method Including Experimental Validation," *IEEE Transactions on Industry Applications*, vol. 35, pp. 790-802, 1999.
- [3] J. F. Bangura and N. A. Demerdash, "Diagnosis and Characterization of Effects of Broken Rotor Bars and Connectors in Squirrel-Cage Induction Motors by a Time-Stepping Coupled Finite Element-State Space Modeling Approach," *IEEE Transactions on Energy Conversion*, vol. 14, pp. 1167-1175, 1999.
- [4] J. F. Bangura and N. A. Demerdash, "Comparison Between Characterization and Diagnosis of Broken Bars/End-Ring Connectors and Airgap Eccentricities of Induction motors in ASDs Using a Coupled Finite Element-State Space Method," *IEEE Transactions on Energy Conversion*, vol. 15, pp. 48-56, 2000.
- [5] J. F. Bangura and N. A. Demerdash, "Simulation of Inverter-Fed Induction Motor Drives with Pulse-Width Modulation by a Time-Stepping Coupled Finite Element-Flux Linkage-Based State Space Model," *IEEE Transactions on Energy Conversion*, vol. 14, pp. 518-525, 1999.
- [6] M. E. H. Benbouzid, "Bibliography on Induction Motors Faults Detection and Diagnosis," *IEEE Transactions on Energy Conversion*, vol. 14, pp. 1065-1074, 1999.
- [7] M. Haji and H. A. Toliyat, "Pattern Recognition - A Technique for Induction Machines Rotor Fault Detection "Eccentricity and Broken Bar Fault", " *IEEE-IEMDC*, 2001.
- [8] R. R. Schoen, B. K. Lin, T. G. Habetler, J. H. Schlag, and S. Farag, "Unsupervised, on-line system for induction motor fault detection using stator current monitoring," *IEEE Transactions on Industry Applications*, vol. 31, pp. 1280-1286, 1995.
- [9] J. F. Bangura, R. J. Povinelli, N. A. O. Demerdash, and R. H. Brown, "Diagnostics of Eccentricities and Bar/End-Ring Connector Breakages in Polyphase Induction Motors through a Combination of Time-Series Data Mining and Time-Stepping Coupled FE-State Space Techniques," presented at IEEE Industry Application Society 2001 Annual Meeting, 2001.
- [10] R. J. Povinelli, J. F. Bangura, N. A. O. Demerdash, and R. H. Brown, "Diagnostics of Bar and End-Ring Connector Breakage Faults in Polyphase Induction Motors Through a Novel Dual Track of Time-Series Data Mining and Time-Stepping Coupled FE-State Space Modeling," presented at IEEE International Electric Machines and Drives Conference (IEMDC 2001), Cambridge, Massachusetts, 2001.
- [11] R. J. Povinelli, J. F. Bangura, N. A. O. Demerdash, and R. H. Brown, "Diagnostics of Faults in Induction Motor ASDs Using Time-Stepping Coupled Finite Element State-Space and Time Series Data Mining Techniques," presented at Third Naval Symposium on Electric Machines, 2000.
- [12] F. M. Roberts, R. J. Povinelli, and K. M. Ropella, "Identification of ECG Arrhythmias using Phase Space Reconstruction," presented at Principles and Practice of Knowledge Discovery in Databases (PKDD'01), Freiburg, Germany, 2001.
- [13] J. F. Bangura and N. A. O. Demerdash, "Effects of Broken Bars/End-Ring Connectors and Airgap Eccentricities on Ohmic and Core Losses of Induction Motors in ASDs Using a Coupled Finite Element-State Space Method," *IEEE Transactions on Energy Conversion*, vol. 15, pp. 40-47, 2000.
- [14] F. Takens, "Detecting strange attractors in turbulence," presented at Dynamical Systems and Turbulence, Warwick, 1980.
- [15] E. Bradley, "Analysis of Time Series," in *An introduction to intelligent data analysis*, M. Berthold and D. Hand, Eds. New York: Springer, 1999, pp. 167-194.
- [16] H. Kantz and T. Schreiber, *Nonlinear time series analysis*. Cambridge: Cambridge University Press, 1997.
- [17] T. M. Mitchell, *Machine Learning*. New York: McGraw-Hill, 1997.
- [18] B. L. Bowerman and R. T. O'Connell, *Forecasting and time series: an applied approach*, 3rd ed. Belmont, California: Duxbury Press, 1993.
- [19] R. J. Povinelli, J. F. Bangura, N. A. O. Demerdash, and R. H. Brown, "Diagnostics of Bar and End-Ring Connector Breakage Faults in Polyphase Induction Motors Through a Novel Dual Track of Time-Series Data Mining and Time-Stepping Coupled FE-State Space Modeling," *IEEE Transactions on Energy Conversion*, vol. 17, pp. 39-46, 2002.
- [20] R. Hegger, H. Kantz, and T. Schreiber, "Practical implementation of nonlinear time series methods: The TISEAN package," *Chaos*, vol. 9, 1999.
- [21] A. Webb, *Statistical Pattern Recognition*. New York: Oxford University Press, 1999.
- [22] D. G. Manolakis, V. K. Ingle, and S. M. Kogon, *Statistical and Adaptive Signal Processing*: McGraw Hill, 2000.
- [23] J. G. Proakis and D. G. Manolakis, *Digital Signal Processing*, Third ed: Prentice Hall, 1996.